ASEAN Journal of Chemical Engineering 2025, Vol. 25, No. 1, 147 – 171

Changes in Dissolved Organic Matter by Fluorescence Excitation-Emission Matrix Analysis during Palm Oil Mill Effluent Treatment Using Dielectric Barrier Discharge

Reni Desmiarti [1]
Maulana Yusup Rosadi [2]
Erda Rahmilaila Desfitri [1]
Joni Aldila Fajri [3]
Nofri Naldi [1]
Muhammad Miftahur Rahman [4]
Ariadi Hazmi [*,5]
[1] *Department of Chemical Engineering, Universitas Bung Hatta, Padang 25147, Indonesia.*
[2] *Department of Civil Engineering, Universitas Borobudur, Jakarta 13620, Indonesia.*
[3] *Department of Environmental Engineering, Universitas Islam Indonesia, Yogyakarta 55584, Indonesia.*
[4] *Graduate School of Engineering, Department of Engineering Science, Gifu University, Japan.*
[5] Department of Electrical Engineering, Universitas Andalas, Padang 25166, Indonesia
e-mail: ariadi@eng.unand.ac.id

Submitted 16 January 2025 *Revised* 9 April 2025 *Accepted* 12 April 2025

Abstract. This study explored the treatability of dissolved organic matter (DOM) in palm oil mill effluent (POME) by dielectric barrier discharge (DBD) treatment under aerated and non-aerated conditions at different electric voltages of 15, 20, and 25 kV. The DOM composition was monitored by fluorescence excitation-emission matrix (EEM) analysis, and tryptophan-like Peak 2 and humic-like Peak 5 were dominant in POME. Chemical oxygen demand (COD), biochemical oxygen demand (BOD), and total solids (TS) were significantly removed by DBD treatment under aerated and non-aerated conditions by 93–98%, 96–98%, and 78–83%, respectively. The relative changes Peak 3/Peak 2 revealed the DOM treatability by DBD treatment, where more protein-like substances were reduced than humic-like substances, owing to the different composition interaction against the oxidation reaction performed by reactive species (O_3, •OH, H_2O_2) generated from the DBD reactor. In contrast, humic-like substances increased after DBD treatment under aerated and non-aerated conditions. Fluorescence indices demonstrated that DBD treatment caused significant changes in the fluorescence index (FI), while no significant changes were observed in the humification index (HIX) and biological index (BIX). This study provides useful information on the changes in DOM from POME after DBD treatment, evaluated by fluorescence EEM analysis.

Keywords: Dielectric Barrier Discharge, Dissolved Organic Matter, Fluorescence EEM Analysis, Humic-like Substances, Palm Oil Mill Effluent.

INTRODUCTION

Palm oil mill effluent (POME) refers to the wastewater generated during palm oil production through several stages, including sterilization, threshing, digestion, pressing,

DOI: 10.22146/ajche.19376

clarification, and drying. It is reported that around 600–700 L/tons of POME were generated from the Indonesian palm oil industry and existed in forms of high total solids (TS), chemical oxygen demand (COD), biochemical oxygen demand (BOD), oil, and grease (ESDM, 2022; Desmiarti *et al.,* 2022). In a summary by Yusof *et al.* (2023), COD in POME varied between 50,000–150,000 mg/L and the BOD value of 25,000–75,000. POME also contains nutrient-rich substances such as phenolic (5800 mg/L) and lignin (4700 mg/L) (Mohammad *et al.,* 2021). It is clearly stated that POME contains high concentrations of organic pollutants. Yet, unclear information on the composition of dissolved organic matter (DOM) in POME has not been fully explored since DOM can raise concerns about the effectiveness of the physicochemical wastewater treatment.

DOM is one of the major concerns during the POME treatment, and it is highly heterogeneous. It is derived from residual plant debris, other synthetic chemicals, and soluble microbial products released from substrate metabolism and biomass decay. DOM in POME is found to be biodegradable and can form toxic by-products from the decomposition process, such as volatile fatty acids, alcohols, and organic acids (Mahmod *et al.,* 2023; Ahmad *et al.,* 2019). It is reported that aromatic compounds, such as phenol and fulvic acid-like in POME, are recalcitrant and have low biodegradability. Thus, conventional water treatment processes face unsatisfactory removal efficiency (Choi *et al.,* 2017). Various treatment processes are employed to remove or reduce DOM from POME through physicochemical and biological processes to address these concerns. Coagulation has been used to remove the bulk of DOM with relatively higher removal efficiency than filtration and chlorination. COD and BOD were removed by 98% and 96%, respectively, using $FeSO_4.H_2O$ as a coagulant under pH 4.7 (Hossain *et al.,* 2022). However, the complex non-biodegradable contaminants are difficult to remove by conventional treatment processes (e.g., coagulation and chlorination). Therefore, considering the DOM compositions and their treatability during wastewater treatment, a sensitive analytical technique is proposed to see the changes in DOM composition through the advanced treatment process.

Fluorescence excitation-emission matrix (EEM) analysis has been widely used to characterize the compositions of DOM based on the positions of fluorescence peaks that determine the different intensity responses to excitation and emission wavelengths. The DOM in wastewater contains complex components derived from microbial metabolites and micropollutants and is dominated by protein-like and humic-like substances (Li *et al.,* 2020). The position of each fluorescence peak in a fluorescence map could provide some information on the DOM physicochemical properties, such as molecular size, extension of the conjugated system, hydrophobicity, and hydrophilicity. The different characteristics of each fluorescence peak may respond distinctly to the physical, biological, and chemical treatment processes. Humic substances located in lower excitation wavelengths in the fluorescence map consist of a mixture of fulvic acid-like and humic acid-like, making them complex components with hydrophobic and hydrophilic characteristics that are not easily removed by conventional water treatment processes (Rosadi *et al.,* 2023). Humic substances in longer excitation wavelengths consist of hydrophobic characters with a limited aromatic chain

derived from microbial metabolites and are easily removed by coagulation. During the treatment, protein-like substances featured in POME were dominated by tryptophan-like components derived from the soluble microbial product (SMP). It is known that protein-like substances perhaps transform into low molecular weight (MW) after oxidation treatment and cause an increase in the intensity of low MW fractions and the structural changes of protein-like components similar to the humic molecules (Rosadi *et al.,* 2023; How *et al.,* 2017). With the different characteristics in fluorescent components consisting of POME, a different interaction against the water treatment may provide information on DOM's treatability during water and wastewater treatment.

Dielectric barrier discharge (DBD) is one of the non-thermal plasma technologies that generate reactive species (e.g., •OH, O_2, H_2O_2, O_3, etc.) from the physiochemical effects (UV irradiation, ultrasonic wave, thermal radiation, etc.) to have strong interactions with various organic pollutants (Guo *et al.,* 2023; Mouele *et al.,* 2021; Mok *et al.,* 2007). Preliminary studies have shown that the reactive species, such as O_3 and H_2O_2, were generated from the DBD reactor and reduced COD and BOD by 60% and 40%, respectively, by maintaining a low temperature during the treatment (Ma *et al.,* 2020). Maintaining the optimum condition during DBD treatment is crucial to maximizing the productivity of reactive species from the electric charges. Oxidation reactions are performed during DBD treatment involving the reaction of reactive species and organic waste or chemicals in water. Increasing the electric voltage can also increase the generation of reactive species. In a study by Luvita *et al*. (2022), increasing electric voltage from 15 kV to 17 kV demonstrated the high formation of O_3 and H_2O_2 by the ionization, excitation, and dissociation process, thus improving the oxidation process. The study also investigated the fact that the treatment time significantly increased the production of reactive species of O_3 and H_2O_2 due to the accumulation of reactive species that can promote an optimum oxidation process. The DOM in water and wastewater varies in concentration and composition and may behave differently through treatment. O_3, •OH, and H_2O_2 in water generated during DBD treatment react selectively with certain moieties of DOM through electron-rich carbon-carbon double bonds on O_3 and •OH radical reactions and the reactivity of hydrophobic and hydrophilic organic acids (Mouele *et al*., 2020; Wert *et al*., 2009). The previous studies observed that the aromatic constituents of DOM and electron-enriched aromatics were preferentially reactive with O_3 than aliphatic carbon content (Lim *et al.,* 2022; Hao *et al*., 2021). These findings provided useful information on how the reactive species interacted with certain DOM characteristics. However, the interaction between reactive species generated from the DBD reactor and the fluorescence peaks determined from the fluorescence EEM analysis has not been fully explored.

The fluorescent DOM has been observed in various municipal and industrial wastewater effluent from paper mills, oil refineries, slaughterhouses, and others (Hao *et al.,* 2021; Louvet *et al.,* 2013; Rodríguez-vidal *et al.,* 2020). However, less information on the DOM composition from POME was assessed by fluorescence EEM analysis. It should be noted that POME poses harmful contaminants that can deteriorate the water quality once it is discharged without proper treatment. A comprehensive evaluation for monitoring the changes in DOM composition

in POME shall be addressed from a better understanding of the POME treatability using DBD treatment. Although the fluorescent components overlap among industries and are difficult to identify as a fingerprint for a specific industrial sector, POME's abundant humic and protein substances may have unique characteristics and treatability against the DBD treatment. This study investigated the role of DBD treatment in reducing and monitoring the changes in DOM composition containing POME using fluorescence EEM analysis. The system was established under aerated and non-aerated conditions at different electric voltages of 15, 20, and 25 kV. The bulk DOM evaluated by COD and BOD was investigated and showed significant changes, followed by a reduction in fluorescent components after DBD treatment.

MATERIALS AND METHODS

POME Used in This Study

POME was collected from the primary sedimentation tank in a wastewater treatment facility in a palm oil company in Indrapura, West Sumatra, Indonesia. POME was screened to remove dirt, plant cell debris, fibers, and other solids before the experiment and was subjected to water quality analysis described later in 2.3; the remaining part of POME was used for the DBD treatment experiment.

The Experiment of DOM Changes in POME by DBD Treatment

DBD treatment was working under aerated (a) and non-aerated (b) conditions and is shown in Figure 1. 800 mL POME was introduced into both aerated and non-aerated reactors, and air was supplied using the Silent β-120 air pump (Nisso, Tokyo, Japan) to the aerated reactor with a flow rate of 2.5 L/min. Both reactors were supplied with electric voltages of 15, 20, and 25 kV with the current intensity of 0.8, 0.9, and 1 A, respectively, under controlled room temperature (25°C), atmospheric pressure (1 atm), and reaction time of 120 min following the procedures described previously (Desmiarti *et al.,* 2022). During DBD treatment, energy consumption was evaluated to see the performance under the optimum conditions. The energy consumption is calculated based on Eq. (1).

$$\text{Energy consumption} = \frac{I\ x\ v\ x\ t}{\Delta COD\ x\ V} \qquad (1)$$

where I is the current intensity (A), v is voltage (Volt), t is the time of the DBD process (hour), ΔCOD is the experimental COD reduction (mg/L), and V is the POME volume (mL).

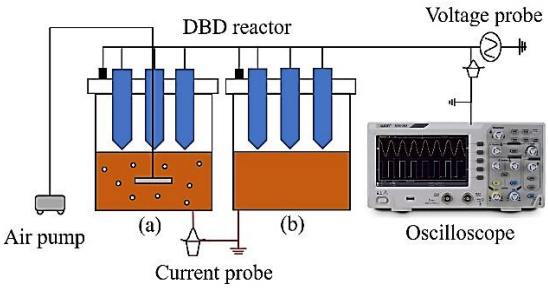

Fig. 1: Schematic procedures of DBD treatment systems working under the aerated condition (a) and non-aerated condition (b).

Water Quality Analysis

COD, BOD, and TS were measured according to the procedures mentioned in the APHA Standard Method (APHA, 2005). For the COD measurement, samples were mixed with solutions containing $HgSO_4$, $K_2Cr_2O_7$, and sulfuric acid and refluxed for 2 h. Titration was performed using ferrous ammonium sulfate (FAS). Samples were dropped with a ferroin indicator into the samples. Titration was immediately stopped when the samples showed a first sharp color

change. COD concentration was calculated based on Eq. (2). For BOD, samples were poured into a dissolved oxygen (DO) bottle and stored in a 20°C incubator for 5 days. DO was measured using a JPB-70A DO meter (Shenzhen Yago Technology, Shenzhen, China) after 5 days of incubation. TS was measured by pouring 100 mL samples into ceramic dishes, drying them at 105°C for 3 hours, cooling them in a desiccator, and weighing the dried samples. The work was repeated until the constant weight value. pH was measured using a HI98107 pH meter (Hanna, Woonsocket, USA), and oxidation-reduction potential (ORP) was measured using a HI98120 ORP meter (Hanna, Woonsocket, USA).

$$\text{COD as } \text{mgO}_2/\text{L} = \frac{(\text{A}-\text{B}) \text{ x M x } 8000}{\text{mL sample}} \qquad (2)$$

where A is the volume of ferroin solution used for the blank, B is the volume of ferroin solution used for samples, M is the molarity of the ferroin solution, and 8000 is the milliequivalent weight of oxygen times 1000 mL/L.

Fluorescence EEM analysis was done with the RF-6000 spectrofluorometer (Shimadzu, Tokyo, Japan). Fluorescence peaks obtained in this measurement were determined using the peak-picking method and can be classified into protein-like and humic-like peaks, as shown in Table 1. The inner filter correction was done automatically after measurement using the corresponding correction function. The excitation (Ex) and emission (Em) wavelengths were set from 220 to 550 nm with a scanning interval of 5 nm. The fluorescence data were stored as the fluorescence intensity in arbitrary units (AU) within the Ex/Em wavelength range.

Table 1. Description of fluorescent components found in this study was determined by the peak-picking method

Peak	Components	Excitation wavelength (Ex)	Emission wavelength (Ex)	Possible sources	References
Peak 1	Protein-like (tyrosine-like)	225 nm	295 nm	Amino acids-tyrosine	Bridgemana *et al.,* 2013; Hudson *et al.,* 2007; Rosadi *et al.,* 2020; Rodríguez-vidal *et al.,* 2021
Peak 2	Protein-like (tryptophan-like)	230 nm	345 nm	Amino acids-tryptophan	Bridgemana *et al.,* 2013; Hudson *et al.,* 2007; Rosadi *et al.,* 2020; Rodríguez-vidal *et al.,* 2021
Peak 3	Humic-like, fulvic-like	225 nm	425 nm	Terrestrial humic	Bridgemana *et al.,* 2013; Hudson *et al.,* 2007; Rosadi *et al.,* 2020; Rodríguez-vidal *et al.,* 2021
Peak 4	Protein-like (tryptophan-like)	270 nm	350 nm	Microbial-derived amino acids-tryptophan	Bridgemana *et al.,* 2013; Hudson *et al.,* 2007; Rosadi *et al.,* 2020; Rodríguez-vidal *et al.,* 2021
Peak 5	Humic-like	330 nm	430 nm	Microbial-derived humic	Bridgemana *et al.,* 2013; Hudson *et al.,* 2007; Rosadi *et al.,* 2020; Rodríguez-vidal *et al.,* 2021
Peak 6	Humic-like	320 nm	390 nm	Microbial-derived humic	Du et al., 2017
Peak 7	Humic-like	495 nm	515 nm	Conjugated humic (wastewater humic)	Du et al., 2017

The humification index (HIX) was used to indicate the degree of DOM humification, with a high HIX value (10–16) indicating strongly humified organic matter from the terrestrial origin. At the same time, a low HIX (<4) indicates freshly produced DOM in the system. HIX was calculated as the area under the emission wavelength of 435–480 nm divided by the sum of the 200–345 nm emission wavelength and 435–480 nm at the excitation wavelength of 255 nm (Qiao *et al.,* 2021). The fluorescence index (FI) indicates the microbial or terrestrial source of DOM, with a high FI value (>1.9) indicating microbial sources and a low FI value (<1.4) indicating a terrestrial and soil source. FI was calculated as the fluorescence intensity ratio of 470 nm and 520 nm emission wavelengths at the excitation wavelength of 370 nm (McKnight *et al.,* 2001). The biological index (BIX) was used to determine the freshness of DOM, with a high BIX value (>1) indicating the newly produced DOM from microbial activities and a low BIX value (0.6–0.7) indicating low DOM production. BIX was calculated as the ratio of the emission wavelength of 380 nm to that of 430 nm using the excitation wavelength of 310 nm (Lidén *et al.,* 2017). Peak 3/Peak 2 was calculated as the intensity ratio of humic-like Peak 3 and protein-like Peak 2, and the value indicates the aromaticity and treatability of DOM (Rosadi *et al.,* 2023).

The humification index (HIX) was used to indicate the degree of DOM humification, with a high HIX value (10–16) indicating strongly humified organic matter from the terrestrial origin. At the same time, a low HIX (<4) indicates freshly produced DOM in the system. HIX was calculated as the area under the emission wavelength of 435–480 nm divided by the sum of the 200–345 nm emission wavelength and 435–480 nm at the excitation wavelength of 255 nm (Qiao *et al.,* 2021). The fluorescence index (FI) indicates the microbial or terrestrial source of DOM, with a high FI value (>1.9) indicating microbial sources and a low FI value (<1.4) indicating a terrestrial and soil source. FI was calculated as the fluorescence intensity ratio of 470 nm and 520 nm emission wavelengths at the excitation wavelength of 370 nm (McKnight *et al.,* 2001). The biological index (BIX) was used to determine the freshness of DOM, with a high BIX value (>1) indicating the newly produced DOM from microbial activities and a low BIX value (0.6–0.7) indicating low DOM production. BIX was calculated as the ratio of the emission wavelength of 380 nm to that of 430 nm using the excitation wavelength of 310 nm (Lidén *et al.,* 2017). Peak 3/Peak 2 was calculated as the intensity ratio of humic-like Peak 3 and protein-like Peak 2, and the value indicates the aromaticity and treatability of DOM (Rosadi *et al.,* 2023).

Data Analysis

The significant differences between the observed data obtained in this study were analyzed by one-way analysis of variance (ANOVA) with a confidence level of 95% ($p = 0.05$) using IBM SPSS Statistics 21.0.

RESULTS AND DISCUSSION

POME Characteristics

Table 2 shows that raw POME contains 7210.5 mg/L COD, 3180.5 mg/L BOD, and 2222 mg/L TS, which is comparatively lower than the previous studies (Akhbari *et al.,* 2019; Foong *et al.,* 2021). However, in some findings, POME contained lower COD, BOD, and TS than ours (James *et al.,* 2023; Shairah *et al.,* 2015). The finding indicates that POME characteristics depend on the quality of the

raw materials and the production processes. Although the concentrations of COD and BOD in this study are lower than those previously reported, the DOM compositions reflected by those two parameters are considerably affected by the effectiveness of the selected treatment processes (coagulation, chlorination, and oxidation).

Table 2. Characteristics of POME in this study. The values in the table are shown as mean values with the standard deviations (n = 3).

Parameters	Values
pH	4.3 ± 0.67
ORP (mV)	-155 ± 119.6
DO (mg/L)	1.08 ± 0.07
COD (mg/L)	7210.5 ± 560
BOD (mg/L)	3180.5 ± 241.2
TSS (mg/L)	2222 ± 192.5
Peak 1 (AU)	455 ± 39
Peak 2 (AU)	804 ± 58.7
Peak 3 (AU)	856 ± 36.6
Peak 4 (AU)	857 ± 24
Peak 5 (AU)	914 ± 80.8
Peak 6 (AU)	659 ± 33.3
Peak 7 (AU)	857 ± 35

Fluorescent DOM components extracted from the fluorescence peak-picking method revealed that seven identified components had characteristics for fluorescence derived from humic and protein substances, which are commonly found in freshwater and wastewater (Rosadi *et al.,* 2023; Rodríguez-vidal *et al.,* 2021). Peak 1 describes the tyrosine-like components derived from soluble microbial products (SMP) with less content of aromatic rings in their structures. Peak 2 and Peak 4 are identified as tryptophan-like components and are the most abundant protein-like. Peak 2 contained phenolic moieties in lignin and low-MW protein substances originating from lignin in fibrous materials. Peak 4, which accounted for 16% of the total fluorescent components, is the second most abundant fluorescent DOM and is originally derived from microbial degradation as the soluble microbial by-product (SMP). These two components are also bound in humic structures commonly observed in the landfill leachate and sludge associated with microbial activity (Rosadi *et al.,* 2023; Du *et al.,* 2017; Wu *et al.,* 2019). Peak 5 is the most abundant component of fluorescent DOM, accounting for a large proportion of total variability, and it is thought to be hydrophobic and has large aromatic chains in humic molecules (Li *et al.,* 2020). Peak 5 has the highest fluorescence intensity, indicating the contribution of non-humic materials cited in long excitation wavelengths, which come from POME. The higher intensity of Peak 5 compared to Peak 3 was also observed in pulp mill effluent (Ciputra *et al.,* 2010), supporting the difference in the origin of humic substances between wastewater and natural water. Fluorescent components emitted in the longer excitation wavelength found in this study as Peak 7 are known to have characteristics assigned to the hydrophobic humic-like components with large molecular sizes detected in raw POME and were well identified in municipal wastewater (Li *et al.,* 2020; Du *et al.,* 2017). Peak 7 also sometimes overlaps with the humic-like Peak 5 and shares the humic characteristics found in wastewater, with Peak 7 being more susceptible to the treatment processes than Peak 5. Another component cited in the longer excitation wavelength in the fluorescence EEM is component Peak 6, which also overlaps with humic-like Peak 5. The fluorescent component Peak 6 indicates the presence of soluble microbial humic-like materials and derived recent biological activity. Peak 3 coincides with the mixture of

humic-like and fulvic-like components in the humic substances and has a complex composition originating from soil organic matter, terrestrial plant debris, and microbial processes in water. The complex structure in humic-like components Peak 3 could indicate the DOM treatability in natural systems and throughout the water and wastewater treatment processes due to higher aromaticity and degradability (Li *et al.,* 2020; Xiao *et al.,* 2018).

BOD:COD value in raw POME is 0.44, which indicates that POME contains biodegradable organic matter (Table 3). The value of BOD:COD in this study was comparatively lower than that found in paper mill, oil refinery, and industrial park wastewater (Park *et al.,* 2022).

Table 3. DOM composition by COD/BOD and fluorescence indices in POME samples. The values in the table are shown as mean values with the standard deviation (n = 3).

Parameters	Values
COD/BOD	0.65 ± 0.11
HIX	0.96 ± 0.16
FI	1.58 ± 0.512
BIX	1.13 ± 0.20
Peak 3/Peak 2	1.07 ± 0.12

The content of BOD significantly influenced the biodegradability of organic matter because of the different chemical properties of DOM in wastewater, resulting in different treatability in the selected treatment processes. HIX in raw POME indicates the degree of DOM's humification with the content of humic substances. This study observed HIX below 4, indicating a lower extent of humification with the strong autochthonous components and the weak terrestrial humic features in DOM. The lignin-rich content in POME caused the low HIX value, with the addition of the biological process involved in POME. BIX in POME posed a value of 1.13, which characterized DOM as a freshly produced material released into water from the biological/microbial origin. The FI value of 1.58 (FI < 2.0) indicates that DOM was less influenced by microbial transformation and more affected by allochthonous origin. The FI value in POME indicates that DOM majorly contains lignin derivatives with rich conjugated aromatic structures.

Changes in COD, BOD, and TS

DBD treatment caused a significant reduction in COD, BOD, and TS, with the most significant reduction observed under the aerated condition (Figure 2). COD and BOD were removed by > 95% under the aerated and non-aerated conditions at different electric voltages of 15, 20, and 25 kV with a natural pH of 4.3 (Table 4). The generation of reactive species (including O_3 and •OH) by the DBD reactor greatly impacted the COD, BOD, and TS reduction with the increase in the electric voltage. With the increase in electric voltage to 25 kV, COD reduced from the initial concentration of 7210 mg/L to 164 mg/L during 2 hours of treatment due to the decomposition of organic compounds in POME by the generated reactive species. The high concentrations of COD and BOD after treatment under 25 kV are probably due to the different responses of organic matter to oxidation. Another reason could be the presence of resistant organic matter in POME that is hard to oxidize. This could be linked to a high residual of fulvic acid-like substances that were thought to be oxidation-resistant. The findings further support the earlier investigation by Ma *et al.* (2020), where a multi-hole DBD system caused a 40% and 60% reduction for COD and BOD, respectively, after 20 min treatment.

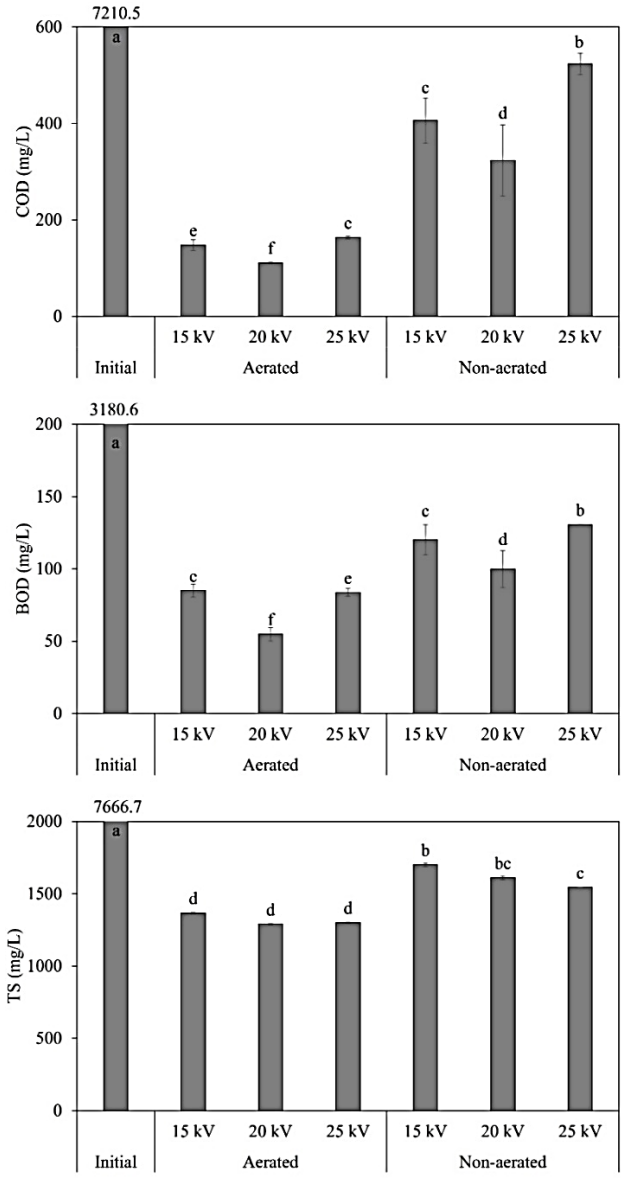

Fig. 2: Changes in COD, BOD, and TS during DBD treatment under the aerated and non-aerated conditions at different electric voltages of 15, 20, and 25 kV. The different letters indicate the observed data are statistically different at $p < 0.05$ (n = 3).

TS gradually decreased from 2167 mg/L to below 1700 mg/L with the increase in electric voltage due to the disruption of the structure of particles in POME. The removal of TS under the aerated conditions was relatively higher (82.2–83.2%) compared to the non-aerated conditions (77.8–79.8%) (Table 4). The presence of oxygen from the supplied air under the aerated condition could assist the reduction in TS as more oxidants are formed to increase the soluble solids in POME. Thus, the removal of TS under the aerated conditions was higher than the non-aerated conditions. The results showed that DBD treatment systems, both under aerated and non-aerated conditions, were responsible for disrupting bulk organic matter by activating oxidants to generate reactive species from the DBD reactor.

Table 4. Average removal of COD, BOD, and TS during DBD treatment under the aerated and non-aerated conditions at different electric voltages of 15, 20, and 25 kV. The values in the table are shown as mean values with the standard deviation (n = 3).

Conditions		Removal percentage (%)		
		COD	BOD	TS
Aerated	15 kV	97.9 ± 0.15	97.3 ± 0.14	82.2 ± 0.04
	20 kV	98.5 ± 0.02	98.3 ± 0.15	83.2 ± 0.03
	25 kV	97.7 ± 0.04	97.4 ± 0.09	83.0 ± 0.04
Non-aerated	15 kV	94.4 ± 0.64	96.2 ± 0.33	77.8 ± 0.05
	20 kV	95.5 ± 0.22	96.9 ± 0.39	79.0 ± 0.16
	25 kV	95.9 ± 0.31	95.9 ± 0.01	79.9 ± 0.13

Changes in Biodegradability Index BOD/COD

The ratio of BOD/COD in raw POME was 0.44 and increased under the aerated condition with a higher enhancement at 15 kV, while a similar value was observed at the electric voltages of 20 and 25 kV (Figure 3). The increase in BOD/COD under the aerated condition indicates parts of new organic substances or intermediate products were transformed into biodegradable products, and some parts were not degraded by the reactive species generated from DBD

treatment. The increase in BOD/COD during DBD treatment under the aerated condition is also attributed to the destruction of molecular structures by reactive species and the degradation of macromolecular-weight organics (such as fulvic and humic acids) into smaller molecular-weight substances (Chen *et al.,* 2019; Jin *et al.,* 2016). Previous studies demonstrated that the decrease in pH indicated the presence of the acid anion by-product from organic substances released after oxidation (Erdem *et al.,* 2020; Dominguez *et al.,* 2019), and the decrease in pH contributed to the increase in BOD/COD.

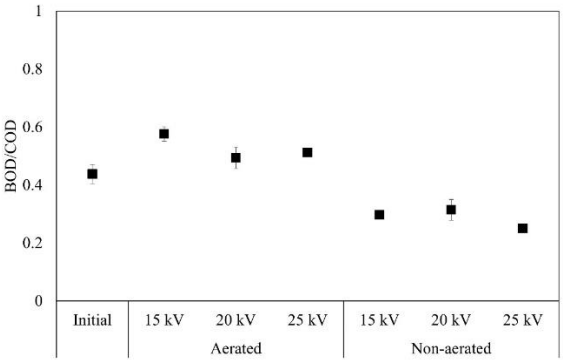

Fig. 3: Changes in the ratio BOD/COD during DBD treatment under the aerated and non-aerated conditions at different electric voltages of 15, 20, and 25 kV ($p < 0.05$, $n = 3$).

However, the pH in this study remained constant after DBD treatment (pH before and after treatment was 4.3–4.7). This might be because the reactive species were not strong enough to degrade organic substances with a complex structure, and the partial oxidation might have occurred and affected only the structure of the aromatic content in DOM molecules, resulting in the formation of low MW with fewer chains of acid-formed organic (Dinçer *et al.,* 2020).

BOD/COD value under the non-aerated condition was 0.30, 0.31, and 0.25 at the electric voltages of 15, 20, and 25 kV, respectively. The result demonstrated that the reduction of BOD/COD under the non-aerated condition indicated that the organic substances in POME were partly converted into slow-degraded substances. Collectively, there were no significant changes ($p > 0.05$) in the difference in electric voltage under the non-aerated condition. The effect of DBD treatment was more pronounced with and without the presence of air. The findings showed that the aerated condition promotes the release of new organic substances. In contrast, the non-aerated condition caused a decrease in BOD/COD, indicating a poor biodegradability of effluent after DBD treatment under the non-aerated condition.

Changes in fluorescent Components of DOM in POME by DBD Treatment

Figure 4 shows that DBD treatment had a good ability to reduce fluorescent DOM in POME. DOM in POME was originally derived from lignin materials that contain more humic-like components and was observed with relatively high intensity. The release of DOM from the bacteria and other particulate matter also influenced the content of protein-like substances with more tryptophan-like components (Zhang *et al.,* 2020; Liu *et al.,* 2022). Fluorescence EEM analysis showed that the fluorescent components in POME decreased markedly with the increase in the electric voltage. DBD treatment caused a significant decrease in all fluorescent components at 25 kV under both aerated and non-aerated conditions. Reactive species (O_3, OH, H_2O_2, etc.) generated from the DBD reactor degraded the fluorophore materials in POME, especially humic substances. Humic substances react faster with the OH radical in water due to their strong redox properties. The supplied air provided oxygen that

assisted the formation of reactive species, such as O_3 and H_2O_2, in POME, which might be more reactive to organic compounds. These radicals also react faster with humic substances in water. Thus, more humic substances (Peak 3 and Peak 5) are reduced than protein-like substances (Salvestrini *et al.,* 2020; García *et al.,* 2020; Hwang *et al.,* 2020).

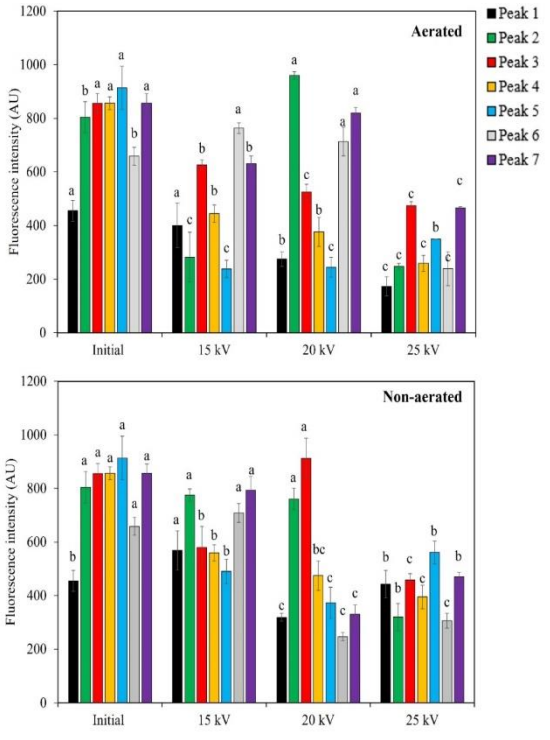

Fig. 4: Changes in fluorescent components during DBD treatment under the aerated and non-aerated conditions at different electric voltages of 15, 20, and 25 kV. The different letters indicate the observed data are statistically different at $p < 0.05$ ($n = 3$)

The oxygen from the air could also maintain the available oxygen to form reactive species to attack more aromatic rings and electron-rich moieties. It is demonstrated that the reduction of humic-like Peak 5, 6, and 7, which are in the emission wavelength above 380 nm, is more susceptible to the DBD treatment at 25 kV under the aerated condition. The finding further confirmed the different characteristics among humic substances from a perspective of their origin and hydrophobicity distribution (Hao *et al.,* 2021), in which humic-like Peaks 5, 6, and 7 perhaps contained high MW humic-like components that have significant oxidation effects compared to that humic-like Peak 3, which remained higher in the residual fluorescence intensity.

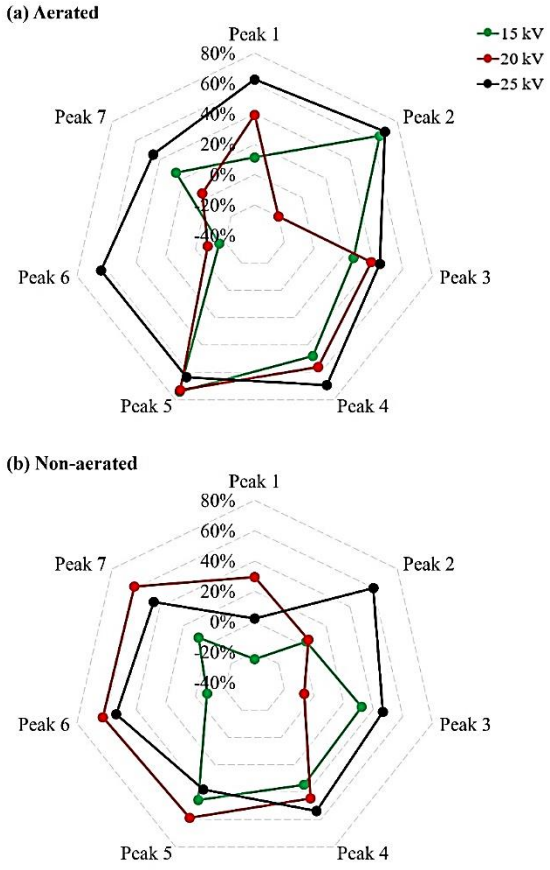

Fig. 5: Average removal of fluorescent components during DBD treatment under the aerated and non-aerated conditions at different electric voltages of 15, 20, and 25 kV ($p < 0.05$; $n = 3$). Top row plots are scaled to a maximum of 80% removal; bottom row plots are scaled to a minimum of -40% removal.

It is known that Peak 3 contains a high portion of fulvic acid-like and is more aliphatic and less aromatic compared to Peak

5 (Ikeya *et al.,* 2020); therefore, Peak 3 is less susceptible to oxidation than Peak 5. There is no significant difference in the removal efficiency of both aerated and non-aerated conditions at 25 kV (Figure 5), demonstrating that both conditions could reduce DOM with or without the presence of oxygen supplied from the air. The higher electric voltage increased the electric field that promoted the ionization, excitation, and dissociation processes in a short time. Thus, DOM was significantly removed under the electric voltage of 25 kV.

Humic-like Peak 3 increased with an enhancement rate of 7% under the non-aerated condition at 20 kV. This result confirmed the insufficient DBD treatment to reduce DOM with complex compositions. The result also shows that the EEM contours of DOM in POME were insignificantly changed, especially humic-like substances, which are indicated with high fluorescence intensity even after treatment (Figure 6). Humic-like Peak 3 is mainly composed of hydrophobic fractions that would be converted into hydrophilic fractions after chemical processes and formed the humic fractions with low MW that are resistant to oxidation (Rosadi *et al.,* 2023; Xiao *et al.,* 2018). These low MW humic fractions caused the increase in the fluorescence intensity of Peak 3 under the non-aerated condition at 20 kV. Another reason is that the generation of reactive species by DBD treatment was not in the maximum phase; thus, the available reactive species only reacted with the part of DOM that contained aromatic structures that were easily attacked by the reactive species. The finding is consistent with the previous observation demonstrating that some parts of humic substances formed after oxidation (Hao *et al.,* 2021; Jin *et al.,* 2016). Notably, the electric voltage influenced the generation of reactive species during DBD treatment. The difference in electric voltage produces the difference in the yield of reactive species and even the species itself. Low electric voltage may yield reactive species with a weak capability to attack organic compounds. For instance, reactive species generated under 15 kV might perform oxidation by attacking fluorophore components' aromatic and conjugated double bonds, but the intermediate products are not mineralized.

This supported our findings that the reduction in humic-like Peak 5 under the aerated and non-aerated conditions yielded the intermediate components defined as humic-like Peak 6 and Peak 7, derived from the freshly produced DOM from the chemical and biological processes.

Protein-like components Peak 2 and Peak 4 constantly decreased with the increase in electric voltage under aerated and non-aerated conditions. The reactive species generated from DBD treatment employed the reaction involving the breakdown of aromatic molecules through halogen substitution that could reduce the fluorescent intensity of protein-like components. However, the decrease in protein-like components was observed for tryptophan-like Peak 4, which had a higher removal than tryptophan-like Peak 2 (Figure 5). The reason behind this is that Peak 4, which is originated from the biological/microbial activity containing a limited number of aromatic rings that are easy to remove in a high portion with the degradation through the oxidation process compared to the tryptophan-like Peak 2 (Hao *et al.,* 2021). The aerated condition caused the increase in tryptophan-like Peak 2 at 20 kV, in which the intermediate products from the mineralization process were formed during DBD treatment. The finding is consistent with the increase in the BIX value (Figure 7),

indicating the presence of the newly formed fluorescent components. Tryptophan-like Peak 2 contained phenolic and amine group fractions, which compose more hydrophobic than hydrophilic features (Xiao *et al.*, 2018). Reactive species such as O_3 available under the aerated conditions of 20 kV might first react with the hydrophobic fractions before hydrophilic ones, yielding more low aromatic features in the hydrophilic fractions (Jin *et al.*, 2016). This can account for the increase in Peak 2 under 20 kV of the aerated condition. A report discussed by Wang *et al.*, 2019 demonstrated that pH affected the de-

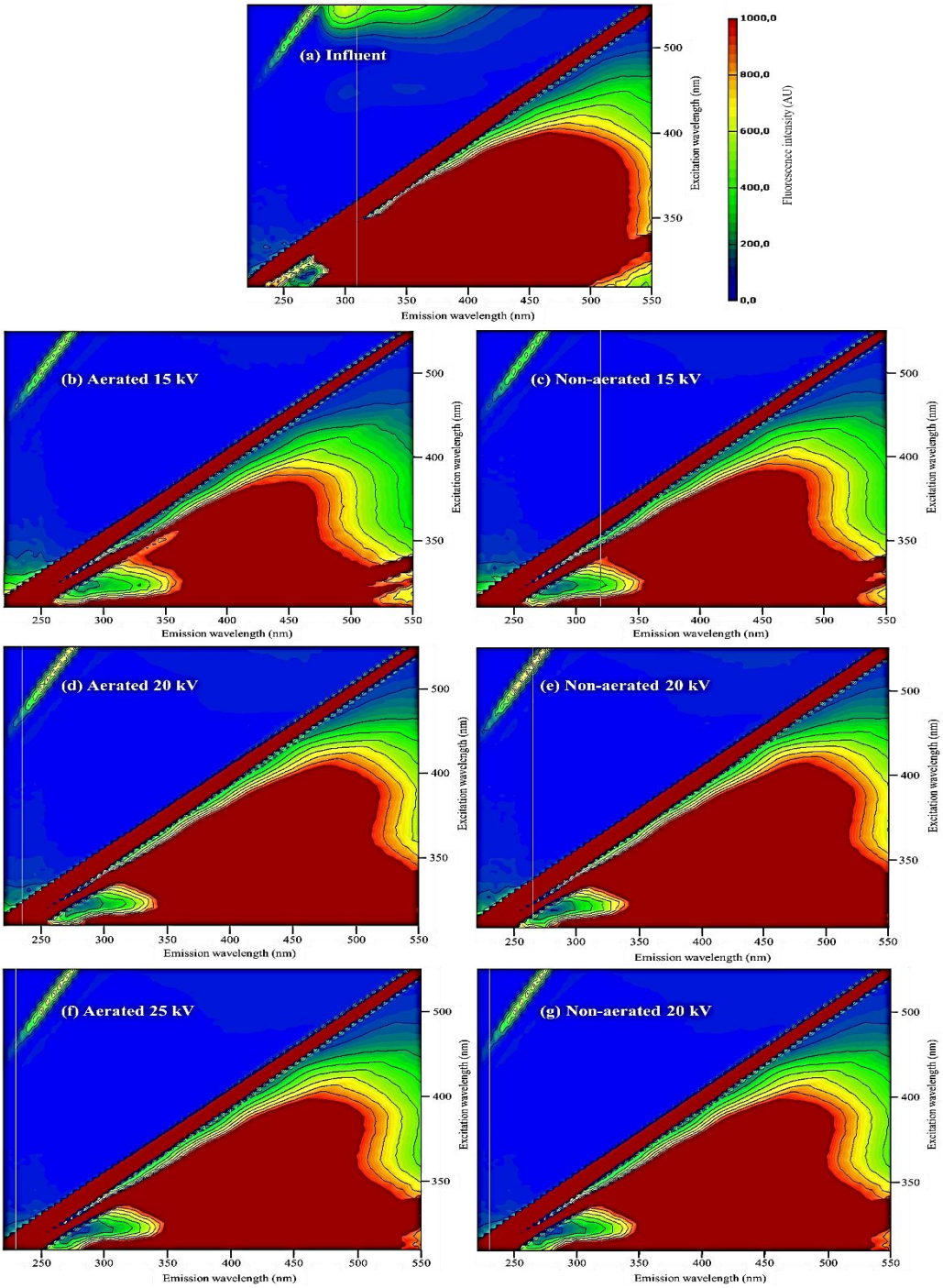

Fig. 6: EEM plot contour of DOM in POME before treatment (a) influent, and after treatment (b–g) under different DBD treatment conditions.

composition of DOM by reactive species, with 7.8 causing oxidation stronger than pH 4. In this study, the non-aerated conditions at 15 and 20 kV had pH 4.3, which might not be sufficient to degrade DOM by reactive species, resulting in insignificant changes in the fluorescence intensity of Peak 2.

The lower intensity of Peak 2 and Peak 4 under 25 kV of both aerated and non-aerated conditions indicates that the reactive species generated during DBD treatment confirmed the decomposition of proteinaceous compounds with the possible mechanism of weakened repulsion interactions between saturated rings in their molecules, making them easily break down into smaller molecules (Wu *et al.,* 2019). In a study by Ge *et al.,* 2022, the presence of O_3 and •OH generated during the ionization process could break down the aromatic structure in DOM and perform the decomposition of proteinaceous content under the anaerobic condition. The significant finding of DBD treatment shows that the aerated conditions at 25 kV reduce more protein-like substances than the non-aerated condition. This indicated that the supplied air led to the higher •OH radicals bound to water under the aerated condition. At the same time, reactive species such as O_3 produced from the DBD reactor increased the formation of H_2O_2 within the solution as the higher electric voltage accelerated plasma formation (Luvita *et al.*, 2022), thus increasing the reactive species' productivities.

Tryptophan-like Peak 4, which was thought to have hydrophobic fractions, reduced significantly in their aromatization degree. Reactive species such as •OH produced a hydrogen-abstraction reaction from C-H bonds of lignin substances but was unsatisfactory for eliminating condensed aromatic protein-like substances (Conde *et al.,* 2023). The presence of reactive species also can perform the electrostatic force between protein-like substances that lowered hydrophobicity through aggregation and precipitation (Zhou *et al.,* 2018), resulting in a consistent decrease in Peak 4 under both aerated and non-aerated conditions. Tyrosine-like Peak 1 with low MW features perhaps converted into refractory hydrophilic fractions and still presented with insignificant changes in the fluorescence intensity after DBD treatment under the non-aerated condition at 25 kV. The removal efficiency of DBD treatment under the aerated condition is substantially higher than that of the non-aerated condition.

The supplied air provided oxygen that assisted the formation of reactive species, such as O_3 and H_2O_2, in POME, which might be more reactive to organic compounds. The oxygen from the air also could maintain the available oxygen to attack more aromatic rings and electron-rich moieties through various processes, such as dissociation, photolysis, and metal-based catalytic reactions (Luvita *et al.,* 2022). The higher electric voltage produced more reactive species and reacted with hydrophobic DOM and then hydrophilic DOM. Reactive species preferentially react with the aromatic features in protein-like molecules through electron-enriched aromatics substituted by oxygen and nitrogen, including phenol and amine groups (Xiao *et al.,* 2018). Thus, Peak 2 decreased significantly owing to the higher aromaticity.

Changes in fluorescence Indices of DOM in POME by DBD Treatment

A higher HIX value in wastewater should lead to the higher removal of DOM by conventional treatment processes, such as coagulation (Figure 7). However, COD was

removed by > 90% using DBD treatment, and it reflected that HIX could not be the indicator for the efficiency treatability by DBD treatment with the HIX value in raw POME at 0.96. HIX increased with increased electric voltages of 15 and 20 kV under the aerated and non-aerated conditions. In contrast, HIX values decreased under both conditions at 25 kV. This indicates that the effect of the electric voltage is more pronounced for the reduction in the humification degree. The reactive species generated at 25 kV could perform the maximum degradation that led to decreased aromatic structures by mineralizing condensed conjugation in fulvic-like fluorescence (Luvita *et al.,* 2022), decreasing HIX value after DBD treatment. The increase in HIX value at 15 and 20 kV indicates the increase in the extent of humification of DOM, which could be attributed to the new formation of DOM that perhaps majorly consisted of humic molecules in the longer wavelength and preferential microbial removal of DOM with labile aliphatic structures and small molecular size which featured similar humic molecules (Li *et al.,* 2020; Rosadi *et al.,* 2023). The results are consistent in the increased fluorescence intensity of tryptophan-like Peak 2 and humic-like components Peak 3. Those components pose a complex composition with the overlap of hydrophobic and hydrophilic fractions, and the degradation by reactive species might only degrade hydrophobic fractions, which are thought to be more prone to the oxidation and the breakdown of high MW into low MW fractions that were accounted in the increase of their intensities.

Figure 7 shows the FI value of DOM in POME before DBD treatment was 1.52, indicating the presence of terrestrially derived DOM. The decrease in FI value in all conditions suggested the relative increase of terrestrial DOM during DBD treatment. The increase in FI value under the non-aerated condition at 25 kV confirmed the degradation of DOM due to endogenous generation. The finding also suggests the contribution of the fresh DOM produced from the biological activity in POME during DBD treatment, which was dominated by proteinaceous materials and amino acids, thus increasing FI value.

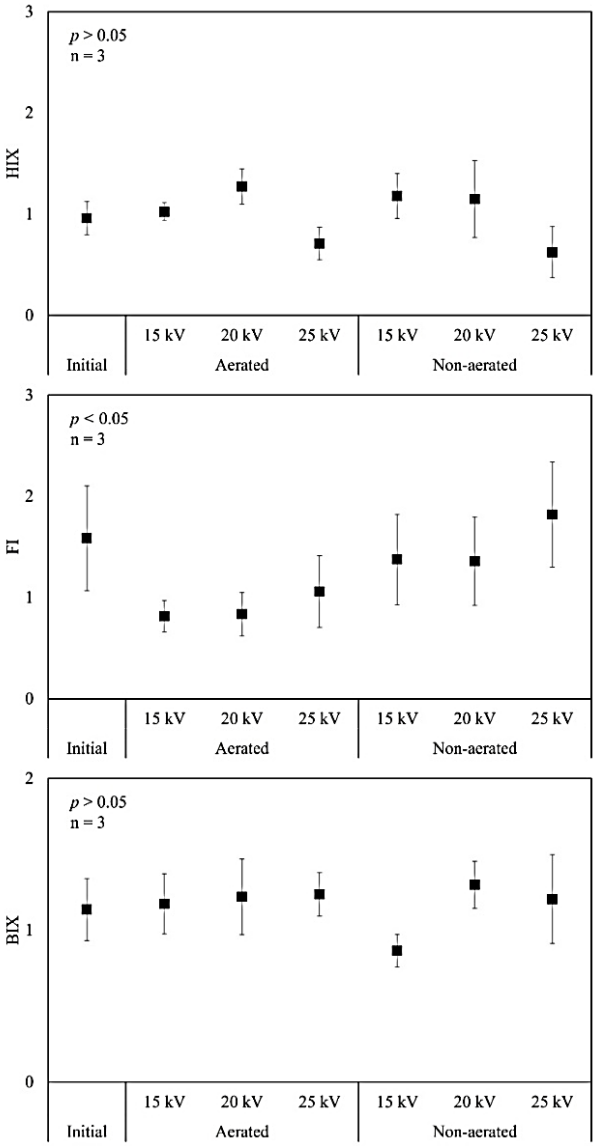

Fig. 7: Changes in HIX, FI, and BIX during POME DBD treatment under aerated and non-aerated conditions at different electric voltages of 15, 20, and 25 kV (n = 3)

The decrease in FI value was consistent with the increase in HIX value, where more terrestrially derived DOM (lignin sources) dominated the composition of DOM in POME after DBD treatment in terms of aerated and non-aerated conditions. DBD treatment caused a slight increase in BIX value above 1 after DBD treatment in all conditions, except under the non-aerated condition with the discharge voltage at 15 kV (Figure 7).

The decrease in BIX indicates the reduction in microbial-derived DOM and easily decomposable organics, leaving the portion of terrestrial-derived DOM in POME under the non-aerated condition at 15 kV. BIX values in all conditions were above 1.0 before and after DBD treatment, suggesting the partial oxidation by reactive species of labile or easily decomposable DOM. The increase in BIX was also thought to be due to the newly formed organic fractions during DBD treatment with low aromatics and low MW, which indicate some stable structure after being oxidized by reactive species during DBD treatment. The finding supported the increased fluorescence intensity of fluorescence DOM in long emission wavelengths (Peak 2, Peak 6, and Peak 7). HIX and FI values suggest that the residual DOM was majorly derived from the terrestrial origin, perhaps from the lignin degradation with low aromaticity in humic molecules. However, the findings were not in line with the increase in BIX value, indicating the contribution of freshly produced DOM by microbial or biological activity (e.g., microbial cell lysis caused by reactive species) after DBD treatment with the content of non-humic fractions. It also should be noted that the increase in BIX value indicates the relative contribution of recently produced DOM and BOD of DOM increases (Chaves *et al*., 2020). The increase in BIX value was inconsistent with the decrease in BOD concentration. Thus, BIX cannot be used as an indicator of the treatability of DOM in POME by DBD treatment.

Changes in Fluorescence Ratio Peak3/ Peak2

Figure 8 shows the changes in fluorescence ratio Peak 3/Peak 2 during 2-hour DBD treatment. Peak 3/Peak 2 describes the DBD treatment capability in explaining the changes in aromatic content in the DOM structure. The index is as relevant as SUVA, indicates aromaticity in water (Rosadi *et al*., 2023).

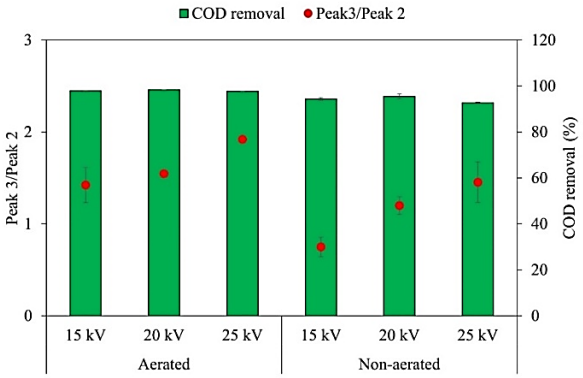

Fig. 8: Correlation between Peak 3/Peak 2 ($p < 0.05$) and COD removal ($p > 0.05$) during DBD treatment under the aerated and non-aerated conditions at different discharge voltages of 15, 20, and 25 kV (n = 3)

Peak 3/Peak 2 increased from the initial value of 1.07 after DBD treatment, demonstrating that DBD treatment removed more protein-like substances than humic-like ones. The finding is inconsistent with the previous study, which described that oxidation preferentially removes humic-like components over protein-like components because aromatic structures in humic-like components are more prone to chemical degradation than protein-like components (Rosadi *et al*., 2023). This could be because

the reactive species generated from the DBD reactor quickly reacted with protein-like components to form chloramine through amino acid chains (Li *et al.,* 2020; Rosadi *et al*., 2023).

Another possibility is the protection of aromatic molecules inside the humic structures that were not directly reacted with the reactive species to perform the decomposition during the partial oxidation of DOM. The results showed that the oxidation treatment proposed by Rosadi *et al*. (2023) and the DBD treatment demonstrated different degradation behavior of Peak 3/Peak 2. The type of DOM exists in freshwater and wastewater, revealing their distinct characteristics. Two possibilities could lead to the changes in this index (increase or decrease of either Peak 3/Peak 2) due to different treatment processes.

The non-aerated condition at 15 kV caused a large decrease in Peak 3/Peak 2, revealing that humic-like components with hydrophobic fractions are reduced by reactive species generated from the DBD reactor. There was an indication that Peak 2 increased under the non-aerated condition at 15 kV. The increase in Peak 2 under that condition resulted in a significant decrease in Peak 3/Peak 2, with a value below 1. The increase in Peak 2 was hypothesized that low and intermediate MW compounds released during the partial oxidation of colloidal matter. The humic-like Peak 3 declined more after DBD treatment under that condition, probably due to susceptible attack by the reactive species, such as O_3 and •OH. Collectively, both the aerated and non-aerated conditions caused the increase in Peak 3/Peak 2. This indicated that the removal of COD was associated with a stronger reduction of protein-like substances by the DBD treatment. In the previous study.

Performance Comparison of DBD with Literature Studies

Energy consumption was evaluated to determine the efficiency of DBD treatment under specific operating conditions. This study found that under the aerated condition, for 120 min at 20 kV and a current intensity of 0.9 A, energy consumption was 0.017 kW.h/mg COD. In contrast, under the non-aerated condition, for 120 min at 25 kV and a current intensity of 1 A, energy consumption was 0.033 kW.h/mg COD. These results indicate that the non-aerated condition required more energy than the aerated condition during DBD treatment. Therefore, further analysis of the operating costs for DBD treatment under both aerated and non-aerated conditions is necessary to provide more accurate and reliable values. Furthermore, the current study demonstrated that the optimal conditions (aerated condition at 20 kV) of DBD treatment resulted in an effluent with COD and BOD concentrations of 111 and 55 mg/L, respectively, which is below the Palm Industry Wastewater Regulation based on the Regulation of Ministry of Environment of the Republic of Indonesia No. 51, 1995. Thus, DBD treatment is a promising technology for treating POME with high pollutant concentrations. Table 5 shows comparative studies of various POME treatments to evaluate their performance under optimal conditions. The results show that different POME treatments achieve varying levels of COD removal under the specified optimal conditions. For instance, while the electro-Fenton demonstrated low energy consumption and high COD removal (Chairunnisak *et al.,* 2018), the need for added electrolytes and H_2O_2 may increase the operational costs. The combination of the electro-Fenton process also demonstrated a

Table 5. Comparative studies of POME treatment

Treatments	Optimum conditions	Performances	References
Electro-Fenton	Current intensity: 3.9 A Voltage: 15.8 V Reaction time: 35.9 min Energy consumption: 0.067 kW.h/mg COD	COD removal: 99.6%	Chairunnisak *et al.,* 2018
Electrocoagulation	pH: 5 Current intensity: 0.45 mA Reaction time: 5 min Energy consumption: 0.10 kW.h/m^3 POME	COD removal: 64% TS removal: 43%	Phalakornkule *et al.,* 2010
Photocatalytic	pH: 5 Current intensity: 0.004 mA Voltage: 0.45 V Reaction time: 6 hr Energy consumption: 1.13 kW.h/m^3 POME	COD removal: 94%	Syahidda *et al.,* 2021
DBD	pH: 4.3 Current intensity: 0.9 A Voltage: 20 kV Reaction time: 120 min Energy consumption: 0.017 kW.h/mg COD	COD removal: 98.5% BOD removal: 98.3% TS removal: 83.2%	This study

good performance in treating POME and required less energy compared to electrocoagulation (Table 5). However, the need for H_2O_2 and ferrous chemicals may also increase operational costs and the possibility of ferric hydroxide precipitation. Combining DBD with other treatments could be a promising technology, such as DBD-ultrafiltration and DBD-adsorption, to treat POME and other wastewater. However, energy consumption, economic outlook, operating conditions, treated effluent quality, and equipment installation must be considered before applying for real wastewater treatment. In addition, since the POME effluent quality after DBD treatment is below the national standard regulation for wastewater, combining DBD treatment with other technologies is unnecessary.

CONCLUSION

This study investigated the changes in DOM during the DBD treatment under the aerated and non-aerated conditions at different discharge voltages at 15, 20, and 25 kV and found that COD, BOD, and TS were significantly reduced by 93–98%, 96–98%, and 78–83%, respectively. Increasing the discharge voltage to 25 kV caused the highest removal efficiency of bulk DOM both under the aerated and non-aerated conditions. The generated reactive species, including O_3, •OH, and H_2O_2, with the presence of dissolved oxygen from the supplied air under the aerated condition, improved the biodegradability and the reduction of fluorescent DOM. Fluorescent DOM changes significantly during DBD treatment, with the highest reduction observed under the aerated condition at 25 kV. This was a result of reactive species reacting more with protein-like substances. Humic-like Peak 5 and tryptophan-like Peak 4 were highly removed by DBD treatment and accounted for 38–74% and 35–69%, respectively, owing to the limited number of aromatic rings that are easy to remove in a

high portion with the degradation through the oxidation process. The relative changes evaluated by Peak 3/Peak 2 increased during the DBD treatment, suggesting the parameter could reflect the performance of DBD treatment under aerated and non-aerated conditions at different discharge voltages. Energy consumption during DBD treatment shows a lower value under the aerated condition (0.017 kW.h/mg COD) than the non-aerated condition (0.033 kW.h/mg COD). The study supports the development of DBD treatment for wastewater treatment by investigating the changes in DOM in POME. However, more exploration should be conducted to investigate the generation of reactive species (including the types and concentration), pH, and temperature. Therefore, a deeper investigation study is necessary by targeting the responsible reactive species on the reduction of DOM in samples from different water and wastewater, including the economic feasibility for the real wastewater application.

ACKNOWLEDGMENTS

This work was supported by the Ministry of Education, Culture, Research, and Technology of the Republic of Indonesia with grant number 186/E5/PG.02.00.PL/2023 and the Department of the Research Program of Higher Education Institution X (LLDIKTI X), Republic of Indonesia with grant number 001/LL10/PG.AK/2023. The authors would like to thank the students of the Department of Chemical Engineering, Universitas Bung Hatta, and the students of the Department of Electrical Engineering, Universitas Andalas, for their assistance in this work.

REFERENCES

A.A. James, M.R. Rahman, D. Huda, M.M. Rahman, J. Uddin, M.K. Bin Bakri, A. Chanda, 2023. "Optimization of novel nanocomposite powder for simultaneous removal of heavy metals from palm oil mill effluent (POME) by response surface methodology (RSM).", *Environ. Dev. Sustain*. 1–27. http://dx.doi.org/10.1007/s10668-022-02849-8

Ahmad, A., Bhat, A.H., Buang, A., Shah, S.M.U., and Afzal, M., 2019. "Biotechnological application of microalgae for integrated palm oil mill effluent (POME) remediation: a review." *Int. J. Environ. Sci. Technol. 16*, 1763–1788. https://doi.org/10.1007/s13762-018-2118-8

Akhbari, A., Kutty, P.K., Onn, C.C., and Ibrahim, S., 2019. "A study of palm oil mill processing and environmental assessment of palm oil mill effluent treatment." *Environ. Eng. Res. 25(2),* 212-221. https://doi.org/10.4491/eer.2018.452

APHA. 2005. Standard Methods for the Examination of Water and Wastewater. 21st Edition, American Public Health Association/American Water Works Association/Water Environment Federation, Washington DC.

Bridgemana, J., Baker, A., Carliell-Marqueta, C., and Carstea, E., 2013. "Determination of changes in wastewater quality through a treatment works using fluorescence spectroscopy" *Environ. Technol. 34(23),* 37–41. https://doi.org/10.1080/09593330.2013.803131

Chairunnisak, A., Arifin, B., Sofyan, H., Lubis, M.R., and Darmadi, 2018. "Comparative

study on the removal of COD from POME by electrocoagulation and electro-Fenton methods : Process optimization Comparative study on the removal of COD from POME by electrocoagulation and electro-Fenton methods : Process optimization." *IOP Conf. Ser.: Mater. Sci. Eng. 334,* 012026. https://doi.org/10.1088/1757-899X/334/1/012026

Chavesa, R.C., Figueredob, C.C., Boëchatc, I.G., Oliveirad, J.T.M. de, and Björn Gückerc, 2020. "Fluorescence indices of dissolved organic matter as early warning signals of fi sh farming impacts in a large tropical reservoir." *Ecol. Indic. 115*, 106389. https://doi.org/10.1016/j.ecolind.2020.106389

Chen, W., Gu, Z., Wen, P., and Li, Q., 2018. "Degradation of refractory organic contaminants in membrane concentrates from landfill leachate by a combined coagulation-ozonation process Weiming." *Chemosphere 217,* 411-422. https://doi.org/10.1016/j.chemosphere.2018.11.002

Choi, Y.Y., Baek, S.R., Kim, J.I., Choi, J.W., Hur, J., Lee, T.U., Park, C.J., and Lee, B.J., 2017. "Characteristics and biodegradability of wastewater organic matter in municipal wastewater treatment plants collecting domestic wastewater and industrial discharge." *Water (Switzerland) 9(409),* 1-12. https://doi.org/10.3390/w9060409

Ciputra, S., Antony, A., Phillips, R., Richardson, D., and Leslie, G., 2010. "Chemosphere Comparison of treatment options for removal of recalcitrant dissolved organic matter from paper mill effluent." *Chemosphere 81*, 86–91. https://doi.org/10.1016/j.chemosphere.2010.06.060

Conde, J.J., Gonz, A.-R.S., Chen, X., Lu-Chau, T.A., Eibes, G., Pizzi, A., and Moreira, M.T., 2023. "Electrochemical oxidation of lignin for the simultaneous production of bioadhesive precursors and value-added chemicals." *Biomass Bioenergy J. 169,* 106693. https://doi.org/10.1016/j.biombioe.2022.106693

D. Ge, W. Wu, G. Li, Y. Wang, G. Li, Y. Dong, H, Yuan and N. Zhu, 2022. "Application of CaO_2-enhanced peroxone process to adjust waste activated sludge characteristics for dewaterability amelioration: Molecular transformation of dissolved organic matters and realized mechanism of deep-dewatering" *Chem. Eng. J. 437(1),* 135306**.** https://doi.org/10.1016/j.cej.2022.135306

Desmiarti, R., Rosadi, M.Y., Hazmi, A., Rahman, M.M., Naldi, N., and Fajri, J.A., 2022. "Biogas Production from Palm Oil Mill Effluent Using Dielectric Barrier Discharge Integrated with the Aerated Condition." *Water (Switzerland) 14*, 1–15. https://doi.org/10.3390/w14223774

Dinçer, A.R., 2020. "Increasing - BOD 5 / COD ratio of non - biodegradable compound (reactive black 5) with ozone and catalase enzyme combination." *SN Appl. Sci. 2*, 1–10. https://doi.org/10.1007/s42452-020-2557-y

Du, H., and Li, F., 2017. "Characteristics of dissolved organic matter formed in aerobic and anaerobic digestion of excess activated sludge." *Chemosphere 168*, 1022–1031. https://doi.org/10.1016/j.chemosphere.2016.10.108

Erdem, C.U., Ateia, M., Liu, C., and Karanfil, T., 2020. "Activated carbon and organic matter characteristics impact the adsorption of DBPs precursors when chlorine is added prior to GAC

contactors." *Water Res.* 116146. https://doi.org/10.1016/j.watres.2020.116146

Foong, S.Z.Y., Chong, M.F., and Ng, D.K.S., 2021. "Strategies to Promote Biogas Generation and Utilisation from Palm Oil Mill Effluent." *Process Integr. Optim. Sustain. 5*, 175–191. https://doi.org/10.1007/s41660-020-00121-y

García, M., Collado, S., Oulego, P., and Díaz, M., 2020. "The wet oxidation of aqueous humic acids." *J. Hazard. Mater. 396*, 122402. https://doi.org/10.1016/j.jhazmat.2020.122402

Guo, H., Su, Y., Yang, X., Wang, Y., Li, Z., Wu, Y., and Ren, J., 2023. "Dielectric Barrier Discharge Plasma Coupled with Catalysis for Organic Wastewater Treatment: A Review." *Catalysts 13,* 1-22. https://doi.org/10.3390/catal13010010

Hao, Y., Ma, H., Wang, Q., Ge, L., Yang, Y., and Zhu, C., 2021. "Refractory DOM in industrial wastewater: Formation and selective oxidation of AOPs." *Chem. Eng. J. 406*, 126857. https://doi.org/10.1016/j.cej.2020.126857

Hossain, M.S., Rashdi, S. Al, Hamed, Y., Al-Gheethi, A., Omar, F.M., Zulkifli, M., and Ahmad Yahaya, A.N., 2022. "Implementation of FeSO4·H2O as an Eco-Friendly Coagulant for the Elimination of Organic Pollutants from Tertiary Palm Oil Mill Effluent: Process Optimization, Kinetics, and Thermodynamics Studies." *Water (Switzerland) 14,* 1-20. https://doi.org/10.3390/w14223602

How, Z.T., Linge, K.L., Busetti, F., and Joll, C.A., 2017. "Chlorination of Amino Acids: Reaction Pathways and Reaction Rates." *Environ. Sci. Technol. 51*, 4870–4876. https://doi.org/10.1021/acs.est.6b04440

Hudson, N., Baker, A., Ward, D., Reynolds, D.M., Brunsdon, C., Carliell-marquet, C., and Browning, S., 2007. "Can fluorescence spectrometry be used as a surrogate for the Biochemical Oxygen Demand (BOD) test in water quality assessment? An example from South West England" *1,* 149-158. https://doi.org/10.1016/j.scitotenv.2007.10.054

Hwang, T., Nam, S., Lee, J., Koo, J., Kim, E., and Kwon, M., 2020. "Hydroxyl radical scavenging factor measurement using a fluorescence excitation-emission matrix and parallel factor analysis in ultraviolet advanced oxidation processes." *Chemosphere 259,* 127396. https://doi.org/10.1016/j.chemosphere.2020.127396

Ikeya, K., Sleighter, R.L., Hatcher, P.G., and Watanabe, A., 2020. "Chemical compositional analysis of soil fulvic acids using Fourier transform ion cyclotron resonance mass spectrometry" *Rapid. Commun. Mass Spectrom. 34,* 1–11. https://doi.org/10.1002/rcm.8801

J. W. Park, S. Y. Kim, J. H. Noh, Y. H. Bae, J. W. Lee, and S. K. Maeng, 2022. "A shift from chemical oxygen demand to total organic carbon for stringent industrial wastewater regulations: Utilization of organic matter characteristics." *J. Environ. Manag. 305,* 114412 https://doi.org/10.1016/j.jenvman.2021.114412

Jin, P., Jin, X., Bjerkelund, V.A., Østerhus, S.W., Wang, X.C., and Yang, L., 2016. "A study on the reactivity characteristics of dissolved ef fl uent organic matter (EfOM) from municipal wastewater treatment plant during ozonation." *Water Res. 88*, 643–652.

https://doi.org/10.1016/j.watres.2015.10.060

Li, L., Wang, Y., Zhang, W., Yu, S., Wang, X., and Gao, N., 2020. "New advances in fluorescence excitation-emission matrix spectroscopy for the characterization of dissolved organic matter in drinking water treatment: A review." *Chem. Eng. J. 381*. https://doi.org/10.1016/j.cej.2019.122676

Lidén, A., Keucken, A., and Persson, K.M., 2017. "Journal of Water Process Engineering Uses of fluorescence excitation-emissions indices in predicting water treatment efficiency." *J. Water Process Eng. 16*, 249–257. https://doi.org/10.1016/j.jwpe.2017.02.003

Lim, S., Shi, J.L., von Gunten, U., and McCurry, D.L., 2022. "Ozonation of organic compounds in water and wastewater: A critical review." *Water Res. 213*, 118053. https://doi.org/10.1016/j.watres.2022.118053

Liu, Y., Wang, X., and Sun, J., 2022. "Bacterial Transformation and Processing of Diatom-Derived Organic Matter : A Case Study for Skeletonema dohrnii." *Front. Microbiol. 13,* 840564. https://doi.org/10.3389/fmicb.2022.840564

Louvet, J.N., Homeky, B., Casellas, M., Pons, M.N., and Dagot, C., 2013. "Chemosphere Monitoring of slaughterhouse wastewater biodegradation in a SBR using fluorescence and UV – Visible absorbance." *Chemosphere 91*, 648–655. https://doi.org/10.1016/j.chemosphere.2013.01.011

Luvita, V., Sugiarto, A.T., and Bismo, S., 2022. "Characterization of Dielectric Barrier Discharge Reactor with Nanobubble Application for Industrial Water Treatment and Depollution South African Journal of Chemical Engineering Characterization of dielectric barrier discharge reactor with nanobubble application for industrial water treatment and depollution." *South African J. Chem. Eng. 40*, 246–257. https://doi.org/10.1016/j.sajce.2022.03.009

Ma, S., Kim, K., Chun, S., Youn, S., and Hong, Y., 2020. "Chemosphere Plasma-assisted advanced oxidation process by a multi-hole dielectric barrier discharge in water and its application to wastewater treatment." *Chemosphere 243*, 125377. https://doi.org/10.1016/j.chemosphere.2019.125377

Mahmod, S.S.; Takriff, M.S.; AL-Rajabi, M.M.; Abdul, P.M.; Gunny, A.A.N.; Silvamany, H.; Jahim, J.M., 2023. "Water reclamation from palm oil mill effluent (POME): Recent technologies, by-product recovery, and challenges." *J. Water. Process. Eng. 52*, 103488–103502. https://doi.org/10.1016/j.jwpe.2023.103488

Mcknight, D.M., Boyer, E.W., Westerhoff, P.K., Doran, P.T., Kulbe, T., and Andersen, D.T., 2001. "Spectrofluorometric Characterization of Dissolved Organic Matter for Indication of Precursor Organic Material and Aromaticity Spectrofluorometric characterization of dissolved organic matter for indication of precursor organic material and aromaticity." *Limnol. Oceanogr. 46,* 38-48 https://doi.org/10.4319/lo.2001.46.1.0038

Ministry of Energy and Mineral Resources Republic of Indonesia, Palm oil mill effluent has the potential to generate 12,654 MW of electricity in Indonesia (in

Indonesian). https://www.esdm.go.id/id/media-center/arsip-berita/limbah-sawit-di-indonesia-berpotensi-hasilkan-listrik-12654-mw, 2018 (accessed 5 July 2022).

Mohammad, S., Baidurah, S., Kobayashi, T., Ismail, N., and Leh, C.P., 2021. "Palm oil mill effluent treatment processes—A review." *Processes 9*, 1–22. https://doi.org/10.3390/pr9050739

Mok, Y.S., Jo, J.O., Lee, H.J., Ahn, H.T., and Kim, J.T., 2007. "Application of dielectric barrier discharge reactor immersed in wastewater to the oxidative degradation of organic contaminant." *Plasma Chem. Plasma Process. 27*, 51–64. https://doi.org/10.1007/s11090-006-9043-1

Mouele, E. S. M., Myint, M. T. Z., Kyaw, H. H., Tijani, J. O., Dinu, M., Parau, A. C., Pana, I. Ouardi, Y. E., Al-Sabahi, J., Al-Belushi, M., Sosnin, E., Tarasenko, V., Zhang, C., Shao, T., Iordache, T. V., Teodor, S., Laatikainen, K., Vladescu, A., Al-Abri, M., Sarbu, A., Braic, M., Braic, V., Dobrestov, S., and Petrik, L. F., 2021. "Degradation of Sulfamethoxazole by Double Cylindrical Dielectric Barrier Discharge System Combined with Ti/C-N-TiO_2 Supported Nanocatalyst." *J. Hazard. Mater. Adv.,* 5, 100051. https://doi.org/10.1016/j.hazadv.2022.100051

Mouele, E.S.M., Tijani, J.O., Masikini, M., Fatoba, O.O., Eze, C.P., Onwordi, C.T., Myint, M.T.Z., Kyaw, H.H., Al-Sabahi, J., Al-Abri, M., Dobretsov, S., Laatikainen, K., and Petrik, L.F., 2020. "Spectroscopic Measurements of Dissolved O 3 , H 2 O 2 and OH Radicals in Double Cylindrical Dielectric Barrier Discharge Technology : Treatment of Methylene Blue Dye Simulated Wastewater." *Plasma 3*, 59–91. https://doi.org/https://doi.org/10.3390/plasma3020007

Pateiro, M., Gagaoua, M., Barba, F.J., Zhang, W., and Lorenzo, J.M., 2019. "A Comprehensive Review on Lipid Oxidation in Meat and Meat Products" *Antioxidants 8*, 1–31. https://doi.org/10.3390/antiox8100429

Phalakornkule, C., Mangmeemak, J., and Intrachod, K., 2010. "Pretreatment of palm oil mill effluent by electrocoagulation and coagulation" *36*, 142–149. https://doi.org/10.2306/scienceasia1513-1874.2010.36.142

Qiao, Z., Hu, S., Wu, Y., Sun, R., Liu, X., and Chan, J., 2021. "Changes in the fluorescence intensity, degradability, and aromaticity of organic carbon in ammonium and phenanthrene-polluted aquatic ecosystems" *RSC Adv. 2,* 1066–1076. https://doi.org/10.1039/d0ra08655j

Rodríguez-vidal, F.J., García-valverde, M., Ortega-azabache, B., González-martínez, Á., and Bellido-fernández, A., 2021. "Using excitation-emission matrix fluorescence to evaluate the performance of water treatment plants for dissolved organic matter removal" *Spectrochim. Acta A Mol. Biomol. Spectrosc. 249,* 119298. https://doi.org/10.1016/j.saa.2020.119298

Rodríguez-vidal, F.J., García-valverde, M., and Ortega-azabache, B., 2020. "Characterization of urban and industrial wastewaters using excitation-emission matrix (EEM) fluorescence: Searching for specific fingerprints" *J. Environ. Manage. 263,* 110396. https://doi.org/10.1016/j.jenvman.2020.110396

Rosadi, M. Y., Maysaroh, S., Sagita, N. D., Anggreini, S., Desmiarti, R., Deng, Z., and Li, F., 2023. "Fluorescence-based Indicators Predict the Performance of Conventional Drinking Water Treatment Processes: Evaluation Based on the Changes in the Compositions of Dissolved Organic Matter." *Chemosphere, 337,* 139410. https://doi.org/10.1016/j.chemosphere.2023.139410

Rosadi, M.Y., Yamada, T., Hudori, H., Tamaoki, H., and Li, F., 2020. "Characterization of dissolved organic matter extracted from water treatment sludge." *Water Sci. Technol. Water Supply 20*, 2194–2205. https://doi.org/10.2166/ws.2020.120

Salvestrini, S., Fenti, A., Chianese, S., Iovino, P., and Musmarra, D., 2020. "Electro-Oxidation of Humic Acids Using Platinum Electrodes : An Experimental Approach and Kinetic Modelling." *Water (Switzerland) 12*, 32–36. https://doi.org/10.3390/w12082250

Shairah, N., Shahrifun, A., Ab'lah, N., Hussain, H., Aris, A., Omar, Q., and Ahmad, N., 2015. "Characterization of Palm Oil Mill Secondary Effluent (Pomse)." *Malaysian J. Civ. Eng. 27*, 144–151. https://doi.org/10.11113/mjce.v27.15914

Syahidda, N., Moksin, A., Por, Y., Ho, L., and Guan, M., 2021. "Optimization of photocatalytic fuel cells (PFCs) in the treatment of diluted palm oil mill effluent (POME)." *J. Water Process Eng. 40*, 101880. https://doi.org/10.1016/j.jwpe.2020.101880

Wang, H., Shen, Y., Lou, Z., Zhu, N., Yuan, H., and Liu, C., 2019. "Hydroxyl radicals and reactive chlorine species generation via E+-ozonation process and their contribution for concentrated leachate disposal." *Chem. Eng. J. 360*, 721–727. https://doi.org/10.1016/j.cej.2018.11.213

Wert, E.C., Rosario-ortiz, F.L., and Snyder, S.A., 2009. "Effect of ozone exposure on the oxidation of trace organic contaminants in wastewater." *Water Res. 43*, 1005–1014. https://doi.org/10.1016/j.watres.2008.11.050

Wu, B., Zhou, K., He, Y., Chai, X., and Dai, X., 2019. "Unraveling the water states of waste-activated sludge through transverse spin-spin relaxation time of low- fi eld NMR." *Water Res. 155*, 266–274. https://doi.org/10.1016/j.watres.2019.02.031

Xiao, K., Shen, Y., Liang, S., Tan, J., Wang, X., Liang, P., and Huang, X., 2018. "Characteristic Regions of Fluorescence Excitation-Emission Matrix (EEM) to Identify Hydrophobic/ Hydrophilic Contents of Organic Matter in Membrane Bioreactors Characteristic Regions of Fluorescence Excitation-Emission Matrix (EEM) to Identify Hydrophobic/Hydrophilic Contents of Organic Matter in Membrane Bioreactors." *Environ. Sci. Technol. 52,* 11251-11258. https://doi.org/10.1021/acs.est.8b02684

Yusof, M. A. B. M., Chan, Y. J., Chong, C. H., and Chew, C. L., 2023. "Effects of Operational processes and Equipment in Palm Oil Mills on Characteristics of Raw palm Oil Mill Effluent (POME): A Comparative Study of Four Mills." *Clean Waste Sys., 5(2),* 100101. https://doi.org/10.1016/j.clwas.2023.100101

Zhang, L., Fang, W., Li, X., Lu, W., and Li, J., 2020. "Strong linkages between dissolved organic matter and the aquatic bacterial community in an urban river."

Water Res. 116089. https://doi.org/10.1016/j.watres.2020.116089

Zhou, H., and Pang, X., 2018. "Electrostatic Interactions in Protein Structure, Folding, Binding, and Condensation." *Chem. Rev. 118,* 1691-1741. https://doi.org/10.1021/acs.chemrev.7b00305